Structure of the Laminar Ablating Air-Teflon Boundary Layer

R. A. GREENBERG,* N. H. KEMP,† AND K. L. WRAY‡
Avco Everett Research Laboratory, Everett, Mass.

Radiation profiles in an ablating flat plate air-Teflon laminar boundary layer have been studied both experimentally and theoretically. The experiments were conducted in a one atmosphere, 3000–6000°K, subsonic freestream produced by an arc jet. Spatially resolved radiation profiles within the boundary layer were obtained in both the visible and infrared. The major radiation in the visible and near ultraviolet wavelengths was the CN violet. In the infrared, the major radiators were CO, CO_2, NO, and COF_2. The theory which was developed to predict the structure included coupling of the heat and mass transfer at the Teflon surface. A partial equilibrium model for the Teflon-air chemistry was utilized, which does not allow the formation of CF_3 and CF_4 within the boundary layer. For the selected wavelengths in the infrared the theory generally predicted quite well both the spatial location and magnitude of the peak radiation, and also predicted the integrated radiation across the layer to within a factor of two. For the selected wavelength in the visible, the radiation intensity, which comes from CN, is much larger than predicted, indicating that CN is not in thermodynamic equilibrium.

Nomenclature

a,b = constants
C = total mass fraction
$\bar{C}$ = nucleus mass fraction in gas
f = stream function
g = dimensionless enthalpy
h = static enthalpy
H = stagnation enthalpy
I = radiation intensity
q = heat-transfer rate
T = temperature
u = x component of velocity
v = y component of velocity
x = distance along surface
y = distance normal to surface
η = Howarth-Dorodnitsyn similarity variable
μ = viscosity
ξ = Howarth-Dorodnitsyn streamwise variable
ρ = density

Subscripts

A = ablation products
e = freestream conditions
i = nucleus
$s0$ = solid cold Teflon
w = wall
0 = leading edge conditions

1. Introduction

ABLATING materials are used extensively to protect hypersonic vehicles from the effects of aerodynamic heating during atmospheric flight. The rate of ablation is generally predicted using boundary-layer theory, which requires solution of the boundary-layer equations. While the predictions of ablation rates are generally in agreement with measurements, no detailed measurements have been made of the structure of the ablating boundary layer itself which could confirm the basic assumptions of the theory. Measurements of velocity or enthalpy are difficult because of the small dimensions of the ablating boundary layer in available high-temperature facilities, and the extremely high temperatures involved. Mor important, polymer or plastic ablators generally react chemically with the high-temperature air, forming new compounds, and alter the temperature and velocity profile; at present there are no measurements of the chemical composition or chemical processes either. However, radiation is emitted from the high-temperature species in the boundary layer. This radiation is of interest since it can be used as a diagnostic tool to yield information on the chemical composition and processes which take place within the boundary layer. The work described here is an experimental and theoretical study of an ablating air-Teflon boundary layer, using spatially resolved radiation at selected wavelengths as the principle diagnostic tool.

The ablating boundary layer was obtained experimentally by passing a subsonic stream of hot air from an arc jet over a flat Teflon plate placed parallel to the stream. The equilibrium temperature of the air was varied from 3000 to 6000°K at one atmosphere pressure. The resulting boundary layer has a hot, subsonic outer edge and a steadily decreasing enthalpy toward the cooler wall. A quantitative discussion of the utility of the present arc jet experiments with respect to flight conditions is given in Ref. 1.

The unique feature of the experiments presented here is the high degree of spatial resolution attained within the boundary layer, which is about 3 mm thick. In the visible region, calibrated spectral plates were used to obtain resolutions of about one-twentieth of the boundary-layer thickness. The infrared data was obtained with a scanning slit coupled to an IR monochromator, which permits spatial resolution of about one-sixth the boundary-layer thickness. Wavelength scans were used to provide information on the radiating species within the boundary layer.

The prediction of radiation profiles provides a very stringent test of a boundary-layer theory since the prediction of the radiation from a point in the boundary layer requires accurate knowledge of the gas composition, temperature, and radiation intensity per particle; however, the concentrations of the radiating species vary by orders of magnitude across the layer, while the radiation intensity per particle is usually

Presented as Paper 69-99 at the AIAA 7th Aerospace Sciences Meeting, New York, January 20–22, 1969; submitted January 28, 1969; revision received October 20, 1969. This research was supported by the Advanced Research Project Agency of the Department of Defense and Space and Missile Systems Organization, Air Force Systems Command and was monitored by Space and Missile Systems Organization, Air Force Systems Command under Contract F04701-68-C-0036. The authors acknowledge many fruitful discussions with M. Camac and G. W. Sutton during this investigation. We wish to thank L. Young for performing many computer calculations of the infrared radiation intensities used in this report. We also acknowledge the assistance of H. Koritz in the experimental program.

* Principal Research Engineer. Member AIAA.
† Principal Research Scientist; now Senior Consulting Scientist, Avco Systems Division, Wilmington, Mass. Associate Fellow AIAA.
‡ Principal Research Scientist.

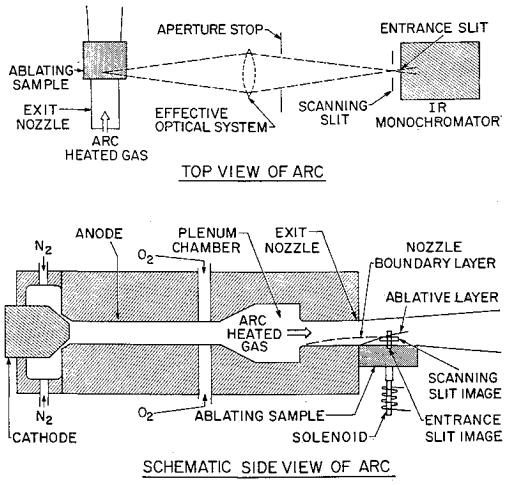

Fig. 1 Sketch of experimental configuration.

strongly temperature dependent. For example, the visible radiation in a high-temperature (~6000°K) air-Teflon boundary layer is primarily due to CN radiation. However, the CN peak concentration is about 10^{-5} of the next more populous radiator in the boundary layer.

The theory employed is the simplest which could be devised that contains the relevant chemistry. The laminar boundary-layer equations are coupled to the Teflon surface through heat and mass balances, using a constant ablation temperature for Teflon. Chemical nonequilibrium effects are taken into account by a partial-equilibrium chemistry model, which does not allow the formation of CF_3 and CF_4. The transport properties of all elements are taken equal, and all Lewis and Prandtl numbers are taken as unity. The presence of a cooled boundary layer on the nozzle upstream of the Teflon plate is taken into account by use of a nonsimilar computational procedure.

A discussion of the methods which were used to obtain the radiation measurements is presented in Sec. 2. There we also discuss measurements which determine the spatial uniformity of the arc freestream and justify the assumption of thermochemical equilibrium. Also, radiation measurements from a pure air boundary layer are compared with a simple boundary-layer theory. Section 3 presents the nonsimilar boundary-layer theory which was used to predict the characteristics of the ablating boundary layer, while Sec. 4 contains a comparison of theory and experiment. Finally, some concluding remarks are presented in Sec. 5.

2. Experimental Methods and Measurements of Air Radiation

Techniques

The design and operation of the arc facility used in the experiments has been described in some detail in Refs. 1–3. The arc generates air at temperatures between 3000 and 6000°K at a pressure of one atmosphere, using about 300 kw of power. Flow velocities are approximately 10^5 cm/sec. The stagnation enthalpy of the heated gas is determined by an energy balance, i.e., by measuring the power supplied to the arc, the power lost to the cooling water, and the flow rates of nitrogen and oxygen. If thermochemical equilibrium is assumed, the gas temperature can be computed; this assumption will be discussed further below.

Figure 1 shows schematically the arc jet and the optical configuration used for observations of the Teflon boundary layer. The external optical system, which had unit magnification, consisted of two 45° mirrors, a 24-in. focal length spherical mirror and an aperture which served as a limiting stop. Visible spectra were obtained with a Hilger f/10 prism spectrograph and a Bausch and Lomb grating monochromator. With a $\frac{1}{4}$ in. aperture, the spatial resolution is 0.13 mm.

For the IR measurements a Perkin-Elmer Model #98 monochromator was used as a dispersion instrument. The radiation from the arc was chopped at about 1000 cps just before entering this instrument (see Fig. 1). The dispersed radiation exiting from the instrument was detected with a liquid nitrogen cooled indium antimonide cell which is sensitive from about 1 to 5.5μ. The detector signal was passed through a 50 cycle band pass filter centered at the chopping frequency before being recorded on an oscilloscope. The electronics were such that the sensitivity of the system was limited by cell noise. The IR monochromator had equal entrance and exit slits which, of course, yielded a triangular wavelength resolution function. The theoretical half width, $\Delta\lambda$, of this resolution function for calcium fluoride optics which were used here has been given by Streiff and Ferriso.[4] Experimental verification of the theoretical resolution function was carried out using several atomic lines in the IR. The wavelength calibration of the instrument was obtained between 1 and 5.5μ by using numerous IR standard absorption bands. Absolute intensity calibration of the entire optical system and detector was accomplished by employing a blackbody source at 500°C.

To obtain spatial resolution in the IR a horizontal scanning slit was placed in front of the entrance slit to the monochromator. The slit was motor driven in a vertical direction as indicated in Fig. 1. The slit was imaged at the vertical plane of symmetry of the arc. In general, the width of this scanning slit was set at 0.25 mm, which was equal to the resolution of the external optical system. The slit was scanned at a velocity of 5 mm/sec, which was compatible with the 50 cycle band pass electronic filter described above. Boundary layers are about 3 mm thick at a station 15 mm downstream from the leading edge of the Teflon block, where most of the measurements were carried out. The result of the geometry of the external optical system and the scanning slit is to produce a net spatial resolution of 0.5 mm in the IR, which is one-sixth of a typical boundary-layer thickness.

For the ablating boundary layer, the radiation intensity was measured at the following wavelengths: 3869 ± 33 Å, 2.48 ± 0.18μ, and 2.90 ± 0.24μ.

Air Radiation Measurements

To check the thermochemical equilibrium assumption and to determine spatial and temporal flow uniformity in the gas, a number of experiments were performed on the freestream. The radiating species were identified and their uniformity across the stream determined by taking spectral plates. Also, quantitative spectral intensity measurements in fixed band passes in both the visible and infrared were compared with theoretical predictions.

Measurements of the absolute intensity in the freestream were made using a calibrated photomultiplier and the monochromator and the external optical system described above. The band pass chosen to make these measurements was 3869 ± 33 Å, since this encompasses the $\Delta v = 0$ sequence of the CN (violet) system, a dominant radiator in the ablating Teflon boundary layer to be discussed below.

The results of these radiation measurements are shown in Fig. 2, along with theoretical calculations which assume the arc heated gas is in thermochemical equilibrium. These results show that the freestream radiation in the temperature range 3500–6000°K can be predicted accurately by equilibrium calculations. For temperatures below 3500°K the theoretical calculations begin to fall below the measured radiation and spectral plates indicate that the gas begins to develop a hot central core. Measured temporal fluctuations in the emission from the hot gas corresponded to temperature

fluctuations of about ±200°K averaged along the optical path perpendicular to the stream. The frequency components of these fluctuations are in the range 20–100 KC. Further measurements were made of the freestream air radiation in the vicinity of 5.3μ, the wavelength of the NO fundamental vibration-rotation band.[3] Both spectral scans and integrated absolute intensity measurements showed excellent agreement with theoretical predictions.

To test our ability to resolve spatially a thin boundary layer, we studied the nonablating boundary layer at the exit plane of the arc nozzle. The Teflon sample shown in Fig. 1 was replaced by a copper plate, and the NO radiation at 5.15μ was observed. Two theories were compared with the experiments, one included a full variable fluid properties boundary-layer solution for nonequilibrium air, the other employed some of the simplifying assumptions used in the ablating boundary-layer theory; thermochemical equilibrium, constant density-viscosity product and unit Prandtl and Lewis numbers. For the latter theory, the momentum equation reduces to the Blasius equation; and since the wall temperature is constant, the solution to the energy equation is given by the Crocco integral.

The radiation per particle in the 5.15 ± 0.18μ band pass is given in Fig. 3, and a comparison of the simple and the full nonequil brium theories with experiment is shown in Fig. 4. The length of the boundary-layer run was taken as 6.25 cm, the length of constant area portion of the nozzle. The external velocity was 10^5 cm/sec, and the wall temperature was 500°K. Considering the uncertainty in the experimental y location of about ±0.1 mm, the agreement between either theory and the experiment seems to be excellent. The effects of any chemical nonequilibrium cannot be determined, since both lines are within the experimental scatter. Additional experiments, performed at other freestream temperatures, showed that above 3600°K the peak radiation was independent of freestream temperature, which confirms the theoretical prediction that the NO radiation peaks within the boundary layer at T = 3600°K. Both the location and magnitude of this peak were predicted very well by both theories.

These boundary-layer experiments show that good spatially resolved radiation profiles can be obtained with the optical system used here; and that a comparatively simple laminar boundary-layer theory predicts this radiation with a high degree of accuracy.

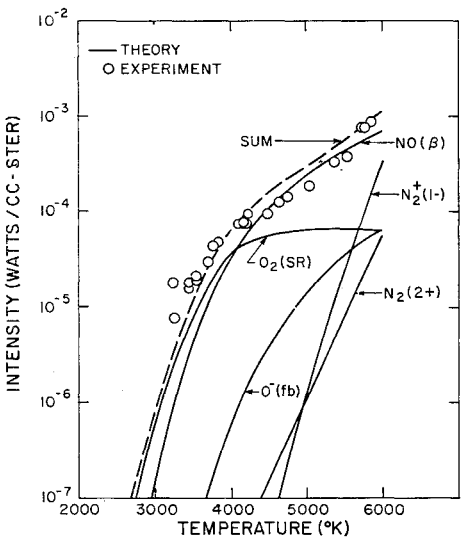

Fig. 2 Freestream radiation from air in the 3869 ± 33 Å bandpass. The solid lines show the individual contributions from various radiators, assuming thermochemical equilibrium.

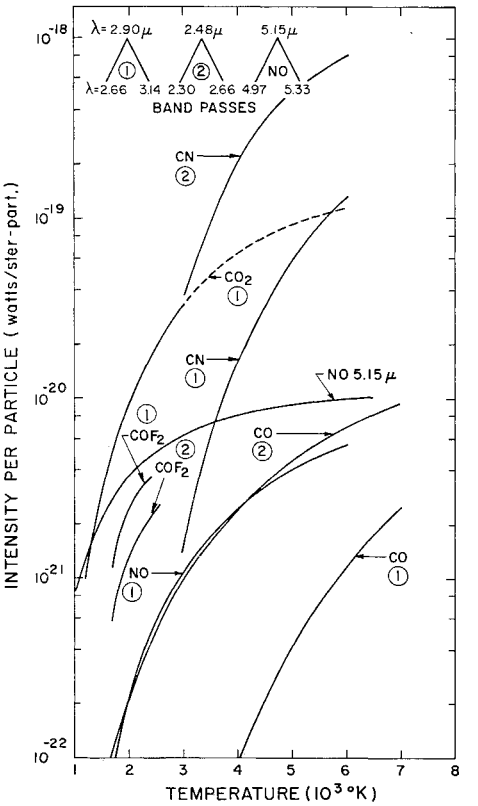

Fig. 3 Radiation intensities per particle in the various band passes.

3. Theory of the Air-Teflon Boundary Layer

The analysis of the ablating layer follows the lines of classical boundary-layer theory except that detailed consideration must be given to the coupling between the ablating surface and the gaseous layer. Both energy and mass balances are made at this interface. Fortunately, the ablation temperature of Teflon is well known, so it is not necessary to construct a complete analysis of the heat transfer within the ablator to obtain a solution to the problem.

Assumptions and Governing Equations

We envisage a boundary layer in which all species have the same value of a given transport property, and all Lewis and Prandtl numbers are unity. Chemical nuclei rather than compounds are followed, which yields the simplification

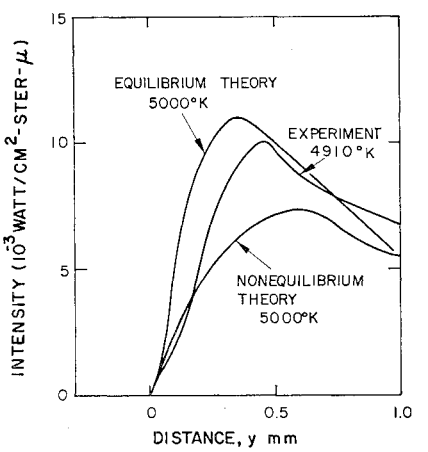

Fig. 4 Radiation from NO in the pure air boundary layer at the nozzle exit (λ = 5.15 ± 0.15 μ; the optical path length is one in.)

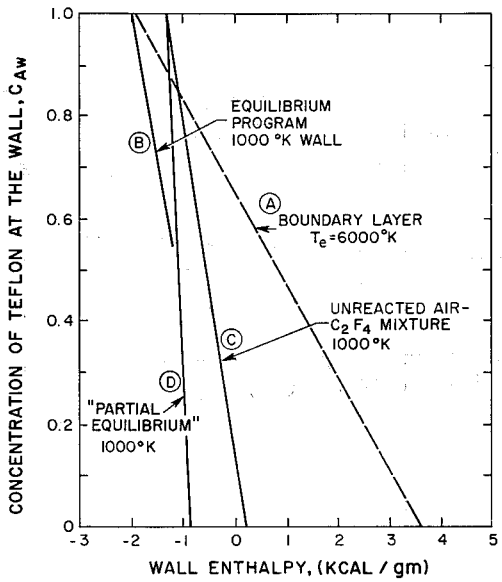

Fig. 5 Various chemical models of the wall state compared to a similar ablating boundary-layer solution of the wall state.

that the conservation of mass relation for each nucleus has no source term, since nuclei are neither created nor destroyed. Fick's law for the diffusion velocity is used. With these assumptions, the relative concentrations of the various nuclei can be obtained simply. Since all nuclei are assumed to have the same diffusivities, the oxygen/nitrogen ratio must be constant across the layer at its free stream value, 0.21/0.79. Similarly, for Teflon, whose empirical formula is C_2F_4, the carbon/fluorine ratio must be $\frac{1}{2}$ across the layer. Thus, it is sufficient to determine only the mass fraction of the ablation mater al, C_A, across the layer. C_A is defined as

$$C_A = \sum_{\text{ablated}} \bar{C}_i = \bar{C}_C + \bar{C}_F \tag{1}$$

where $\bar{C}_i$ is the nucleus mass fraction. With brackets denoting the number of moles per mole of C_2F_4, we obtain the follow.ng expressions for the mole fractions

$$\begin{gathered}[C] = 2,\ [O] = 1.47(1 - C_A)/C_A \\ [F] = 4,\ [N] = 3.72[O]\end{gathered} \tag{2}$$

The governing equations for conservation of momentum, energy, and ablating nuclei are written in terms of the Howarth-Dorodnitsyn independent variables ξ and η

$$\begin{aligned}\xi &= \int_0^x u_e(\rho\mu)_w dx, \\ \eta &= \frac{u_e}{(2\xi)^{1/2}} \int_0^y \rho dy\end{aligned} \tag{3}$$

The subscript w denotes the wall value of $\rho\mu$, which is a function of x. We define the usual dependent variables as

$$f_\eta = u/u_e,\ g = H/H_e \tag{4}$$

where ξ and η subscripts will be used to denote partial derivatives. The conservation equations are,

momentum

$$f_{\eta\eta\eta} + ff_{\eta\eta} = 2\xi(f_\eta f_{\eta\xi} - f_\xi f_{\eta\eta}) \tag{5a}$$

energy

$$g_{\eta\eta} + fg_\eta = 2\xi(f_\eta g_\xi - f_\xi g_\eta) \tag{5b}$$

ablating nuclei

$$C_{A\eta\eta} + fC_{A\eta} = 2\xi(f_\eta C_{A\xi} - f_\xi C_{A\eta}) \tag{5c}$$

The boundary conditions in the freestream are

$$g \to 1,\ f_\eta \to 1,\ C_A \to 0 \tag{6}$$

If we denote the location of the leading edge of the Teflon plate as ξ_0, the boundary conditions on the nozzle wall are, for $0 < \xi \leq \xi_0$

$$\eta = 0,\ g = g_{w0},\ f = 0,\ f_\eta = 0 \tag{7a,b,c}$$

The solutions to the governing Eqs. (5a,b) subject to these boundary conditions are the Blasius solution and the Crocco integral.

For $\xi > \xi_0$ we must perform energy and mass balances at the Teflon surface. The energy balance is obtained by first writing the net heat transfer from the gas to the surface, $-q_{Aw}$, as

$$-q_{Aw} = -q_w - (\rho v)_w h_w + (\rho v)_w h_{Aw}$$

Here $-q_w$ is the heat transfer by conduction and diffusion, and the other two terms represent convection of energy with the gas and ablator enthalpies respectively. For steady-state ablation, $-q_{Aw}$ may also be written in terms of an energy balance within the solid Teflon,

$$-q_{Aw} = (\rho v)_w(h_{Aw} - h_{s0})$$

where h_{s0} is the enthalpy of room temperature solid Teflon. Eliminating q_{Aw} from the above equations yields the appropriate energy balance at the surface

$$-q_w = (\rho v)_w(h_w - h_{s0}) \tag{8}$$

The mass ba ance at the Teflon surface is

$$(\rho v)_w(1 - C_{Aw}) = -(\mu \partial C_A/\partial y)_w \tag{9}$$

In terms of the Howarth-Dorodnitsyn variables, the boundary conditions are

$$g_{\eta w}/(g_{s0} - g_w) = C_{A\eta w}/(1 - C_{Aw}) = f_w + 2\xi f_{\xi w} \tag{10}$$

The Eqs. (5a,b,c) are a seventh-order system with six boundary conditions, given by Eqs. (6, 7c, and 10). The additional boundary condition should involve a balance between the heat transfer within the ablator and its mass loss, which would determine the surface temperature. Since the ablation temperature of Teflon is known to be 1000°K within a few degrees, we employed this value as our additional boundary condition.

Thermodynamic Properties of the Air-Teflon Mixture

The solution of the system of equations and boundary conditions given above yields values for the enthalpy of the mixture and the mole fractions of C, F, O, and N within the boundary layer. To compute the temperature and species profiles, it is necessary to define a chemical model which determines the compounds formed by these elements. The previous results have shown that the radiation from both the freestream and nozzle boundary layer can be predicted within the experimental accuracy by equilibrium theories. For the ablation experiments, the assumption of concentration equilibrium for major species is reinforced by the rapid reactions between carbon compounds and oxygen. The equilibrium composition may be computed by using a thermochemical equilibrium program, which is based on the JANAF tables.[5]

This procedure leads to a formidable complication at the wall where neither C_{Aw} or h_w are known, but T_w is well known for Teflon. The problem is to find values of C_{Aw} and h_w

which satisfy both the equilibrium program, the boundary-layer equations, and the interface conditions, Eq. (10).

It is instructive to consider a simple case to understand this complication. When g_w and C_{Aw} are independent of x, and there is no nozzle boundary layer, the solutions to Eqs. (5b,c) are given by the Crocco integrals,

$$(C_{Aw} - C_A)/C_{Aw} = (g - g_w)/(1 - g_w) = (H - h_w)/(H_e - h_w)$$

These relations may be inserted into the boundary conditions given in Eq. (10) so that the following relation between h_w and C_{Aw} is obtained as a solution to the boundary-layer equations at the wall

$$h_w = H_e - C_{Aw}(H_e - h_{s0}) \tag{11}$$

The quantity h_{s0} is the enthalpy of solid Teflon (C_2F_4) at 300°K. This enthalpy is obtained from Ref. 5–7 as −1.93 kcal/gm. Eq. (11) is shown plotted in Fig. 5 for a freestream temperature of 6000°K as line A. Line A satisfies the boundary-layer equations and the heat and mass balances at the surface. Calculations of h_w vs. C_{Aw} using the equilibrium program based on Ref. 5 for a temperature of 1000°K and 1 atm are shown as Line B in Fig. 5. The wall state should be at the intersection of these two lines, but they do not intersect. Raising the wall temperature to 1100°K would provide an intersection at $C_{Aw} = 1.0$; however, the composition of the gas for C_{Aw} near unity is largely CF_4, CF_3, and solid carbon. Since no solid carbon radiation was experimentally observed, the assumption of complete thermochemical equilibrium does not yield an accurate picture of the gas state at the Teflon surface.

Another possible model for the thermodynamic state of the gas at the wall is an unreacted mixture of C_2F_4 gas and air, both at 1000°K and 1 atm. The results of such a mixture calculation are shown as line C in Fig. 5. Lines C and A do intersect, but if the values of C_{Aw} and h_w at the intersection are used in the equilibrium computations the resulting equilibrium state is at a temperature much greater than 1000°K because the C_2F_4 and O_2 react exothermically. This model would thus produce a temperature discontinuity at the wall, which is also unacceptable.

One way to reconcile the difficulties is to develop a model which predicts C_2F_4 gas at 1000°K as an equilibrium state if $C_{Aw} = 1$. This can be done by considering the kinetic model for C_2F_4 decomposition proposed in Ref. 8, which suggests that the equilibrium composition of curve B, which contains large amounts of CF_4 and CF_3, is not attained in the time scale of our experiments since CF_3 and CF_4 are formed by three body collisions, which are relatively slow. We have, therefore, considered a "partial equilibrium" model in which the compounds CF_3 and CF_4 are deleted from the equilibrium calculation. The results of such a calculation are shown as curve D in Fig. 5. This curve maintains C_2F_4 gas at 1000°K when $C_{Aw} = 1.0$, and it crosses the boundary-layer solution at a reasonable value of C_{Aw}. For C_{Aw} near unity, the gas is found to be a mixture of only three compounds: C_2F_4, COF_2, and N_2; all the oxygen reacts with the C_2F_4 to form COF_2 and the N_2 is unreacted. This partial equilibrium model was used in the numerical calculations presented below.

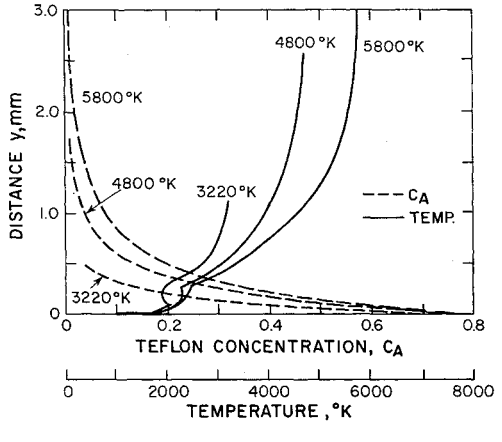

Fig. 6 Theoretical temperatures and Teflon concentrations in the ablating boundary layer at a station 15 mm downstream from the nozzle exit plane.

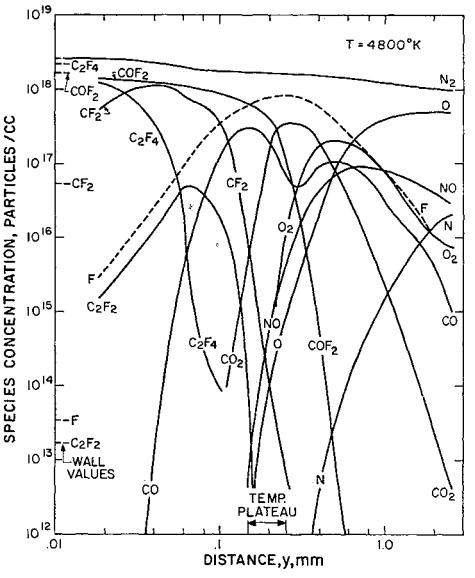

Fig. 7 Theoretical distribution of species in the ablating boundary layer for the partial equilibrium model for T_e = 4800°K.

For the three component mixture which is found at the wall, the enthalpy is a linear function of C_{Aw},

$$g_w = h_w/H_e = (1/H_e)(aC_{Aw} + b) \tag{12}$$

where a = 0.43 kcal/gm, and b = −0.857 kcal/gm. This relation is an analytical representation of the chemical state near the wall, which was utilized in the numerical solutions. The details of these nonsimilar solutions are discussed in Ref. 3.

Theoretical Results

Theoretical calculations were performed for the stream temperatures of 3220, 4800 and 5800°K. The concentration of Teflon as a function of distance normal to the surface is shown in Fig. 6 along with corresponding temperature distributions. As expected, C_{Aw} decreases with freestream temperature, T_e. The Teflon concentration at a given value of y decreases even more rapidly with T_e, because the density is higher in the cooler boundary layer. The temperature distributions of Fig. 6 show an unusual feature. As y increases, there is a temperature plateau at high T_e, which becomes a local minimum at T_e = 3220°K. Of course, the enthalpy always increases monatonically from the surface in our model. Therefore, the plateau must be associated with endothermic chemical reactions occurring in this region of the layer Fig. 7 shows the distribution of reactants within the boundary layer for T = 4800°K; the distance scale is expanded near the wall to clearly show the rapid variations. These results are illustrative of those obtained for the other temperatures. In the temperature plateau region we see peaks in the particle density of fluorine, CO_2 and CO (double peak). We also note that although the mole fraction of C_2F_4 is high at the wall, there are still more molecules of N_2 than C_2F_4. In addition, the particle con-

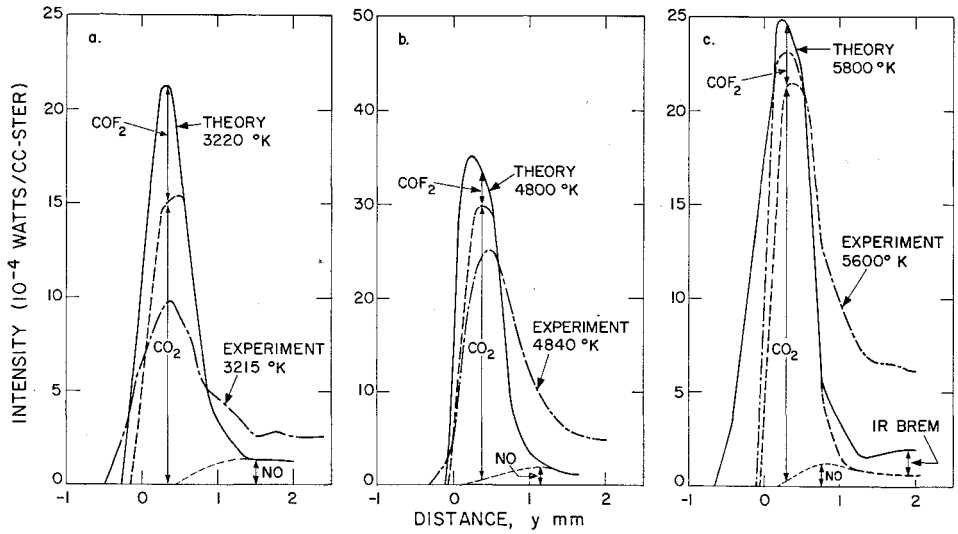

Fig. 8 Theoretical and experimental infrared radiation intensity distributions in the air-Teflon boundary layer; Channel 1 ($\lambda = 2.90 \pm 0.24\mu$).

centration of COF_2 is high near the wall, but it decreases rapidly as we proceed out into the boundary layer.

4. Comparison of Theory and Experiment

Experiments were performed in the freestream temperature range 3000–6000°K. Both visible and IR data were obtained using the techniques discussed in Sec. 2. The results of the theoretical calculations discussed in Sec. 3 were combined with the radiation intensities given in Fig. 3 to determine the theoretical radiation profiles.

Spectra of the air-Teflon boundary layer showed that the radiation in the visible and near UV is dominated by the CN violet system.[1–3] Neither C nor C_2 (Swan) radiation was detected though some runs made with only nitrogen in the freestream showed them to be strong radiators in the nitrogen-Teflon boundary layer. Spatially unresolved wavelength scans of the air-Teflon boundary layer between 2.0 and 3.2μ indicated that the principle radiators were CO_2 ($\nu_1 + \nu_3$), CO_2 ($2\nu_2 + \nu_3$), NO (2ν) and CO (2ν). Of course, these scans also showed the NO (ν), CO (ν), and CO_2 (ν_3) bands in the 4.0 to 5.3μ region. Although COF_2 was not identified in the scans, its possible presence in the spectra could not be eliminated. Since the theory predicts that the COF_2 particle density is high very close to the wall, it was included in the theoretical radiation estimates. Although fluorine is a major component in part of the boundary layer according to the theory, it is not an important radiator.

Figure 8 shows the experimental and theoretical radiation profiles in the 2.90μ ($\Delta\lambda = 0.24\mu$) band pass. The spatial resolution function of the optical instrument has been impressed on the theoretical results to provide a more accurate basis for comparison. The $y = 0$ position of the optical instrument was taken as the point where the leading edge of the resolution function first intersected the surface of the Teflon. However, the data are plotted using the position of the center of the resolution function. Therefore, the radiation begins to rise at values of y less than zero. The peak in radiation is due to CO_2, although COF_2 radiation is important near the surface. At 4800°K and 3220°K the NO radiation dom nates in the outer portion of the boundary layer. The CO radiation contribution is a'ways negligible. We see that both the peak intensity and its location are predicted well by the theory. Beyond the peak, at the higher temperature, the theoretical predictions fall off more rapidly than the experimental data. As a result of this, at 5800°K the theoretical value for the total integrated radiation in this band pass is about a factor of two lower than that obtained experimentally. At 4800°K the theoretical and experimental integrated radiation agrees well, while at 3220°K the theory overpredicts the radiation by about a factor of two. Note that the peak intensity of the CO_2 radiation is weakly dependent up temperature, even though the radiation intensity per particle in Fig. 3 varies by about 10^2 through the layer, while the particle density of CO_2 varies by 10^5 in Fig. 7.

Figure 9 shows the radiation at $\lambda = 2.48\mu$ ($\Delta\lambda = 0.18\mu$) due to CO (2ν), COF_2 and IR Bremsstrahlung. Again the position and magnitude of the radiation peak is predicted well. The COF_2 radiation predicted by the theory before it is modified by the experimental resolution function is highly

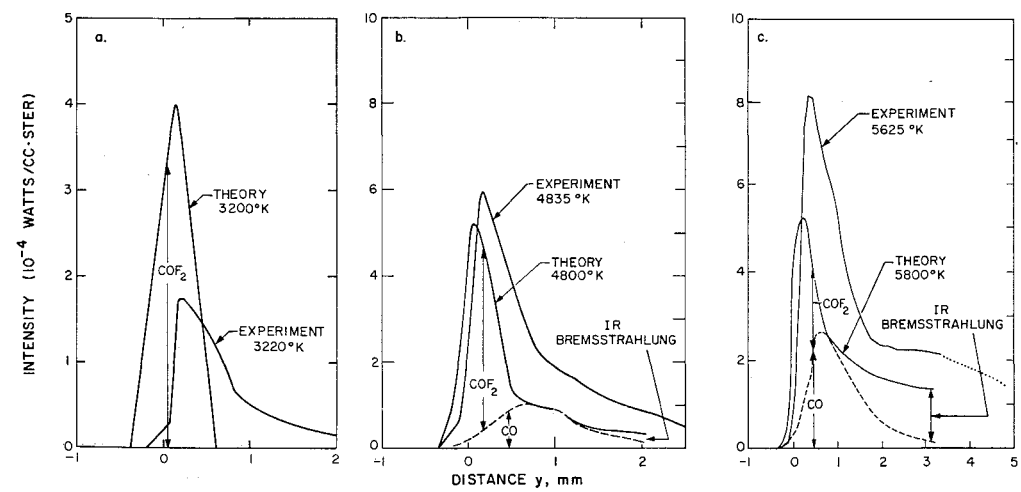

Fig. 9 Theoretical and experimental infrared radiation intensity distributions in the air-Teflon boundary layer; Channel 2 ($\lambda = 2.48 \pm 0.18\mu$).

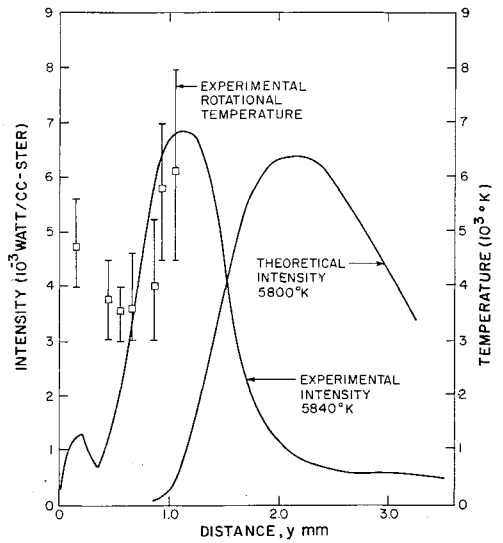

Fig. 10 Visible radiation intensity in the air-Teflon boundary layer, and experimental rotational temperature distribution (λ = 3869 Å).

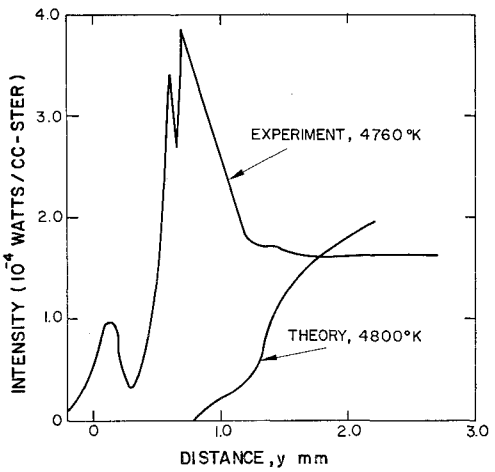

Fig. 11 Visible radiation intensity in the air-Teflon boundary layer (λ = 3869 Å).

peaked at the surface, and decays rapidly until it is negligible about 0.25 mm from the surface. The limited spatial resolution of the IR instrument did not permit us to positively identify the COF_2 radiation. At 3220°K the theory predicts that the most important radiator in the band pass is COF_2. This radiation is about 10^2 times greater than the CO radiation.

The CN (violet) radiation is shown for T = 5800 and 4800°K in Figs. 10 and 11. At 5800°K the peak and total intensity are predicted well, but the location of the peak is twice as far from the surface as the experimental measurement. Also, the second peak near the surface is not predicted. At 4800°K the theory predicts no radiation peak; in fact, the dominant radiator is predicted to be NO(β). The 3200°K result, not shown here, is similar to the 4800°K case. Since the dissociation energy of 7.5 ev for CN is recommended in Ref. 5 with reservations, and this value is somewhat controversial, we also calculated the partial equilibrium concentrations, temperatures, and the resulting radiation for T_e = 5800°K using a value of 8.1 ev for the dissociation energy of CN. Since CN is a trace species in the boundary layer, the temperature is essentially unaffected by the different dissociation energy; however, the CN concentration increases by a factor of three. The CN radiation is increased by this same factor over that shown in Fig. 10, but the shape of the theoretical curve is unchanged. At lower temperatures the increased dissociation energy does not increase the CN radiation significantly.

Also shown in Fig. 10 is the CN (violet) (0,0) rotational temperature profile in the boundary layer, which was obtained by densitometry of a spectral plate.[2] It may be compared with the calculated temperature distribution shown in Fig. 6. At the outer edge of the boundary layer the rotational temperature agrees reasonably well with the calculated temperature. However, instead of decreasing monatonically to the wall temperature, the rotational temperature rises to over 4000°K near the Teflon surface.

The effect is presently unexplained in detail, but might be due to formation of the electronically excited state of CN ($B^2\Sigma$) in high rotational levels which radiate before they can be quenched by collisions. Such a phenomenon is well-documented in the flame spectroscopy literature; for example, the OH radical has yielded rotational temperatures well above the theoretical equilibrium flame temperature.[9] CN, like OH, has a very short radiative lifetime. Kiess and Broida[10] have found anamolous rotational distributions in the CN (violet) radiation from cold flames of atomic nitrogen reacting with halogenated hydrocarbons.

The partial equilibrium model was utilized in the theoretical calculations since it gave a physically acceptable temperature and chemical composition at the wall. However, while it is of interest to note that use of the full equilibrium calculation at the wall did give temperature discontinuities there, the radiation predictions further out in the boundary layer were quite similar to those obtained with the partial equilibrium model.

5. Conclusions

In the previous section we have compared a simple theory which is based on a partial equilibrium chemical model with experimental results. This is a stringent test of the theory, since we require it to predict not the gross features of the boundary layer, such as heat transfer and skin friction, but detailed radiation profiles within the boundary layer. The theory is able to predict the peak intensity of the CO_2 radiation, its position in the boundary layer, and the integrated intensity across the layer to within a factor of two. The peak CO_2 radiation is independent of temperature in the range of our experiment, 3200–6000°K.

The position and magnitude of the 2.48μ radiation peak is predicted well and the theory shows that a substantial portion of this radiation is from COF_2. The individual contributions from COF_2 and CO could not be observed experimentally, because of spatial resolution limitations.

The inability of the theory to explain the visible CN radiation data with comparable accuracy to that in the infrared may well be related to the anomalous CN rotational temperature distribution in the layer. This leads us to the conclusion that even at one atmosphere, the dominant visible and near UV radiation in the air-Teflon boundary-layer experiments comes from CN out of thermodynamic equilibrium.

References

[1] Wray, K. L., Rose, P. H., and Koritz, H. E., "Measurements of the Radiation from an Ablation Contaminated Boundary Layer Under Simulated Flight Conditions," Research Rept. 226, Aug. 1965, Avco Everett Research Lab.

[2] Wray, K. L. and Kemp, N. H., "The Ablating Boundary Layer on a Teflon Plate in an Arc Heated Air Stream," AIAA Paper 66-56, New York, Jan. 1966; also RN 596, Aug. 1966, Avco Everett Research Lab.

[3] Greenberg, R. A., Kemp, N. H., and Wray, K. L., "Structure of the Laminar Ablating Air-Teflon Boundary Layer," Research Rept. 301, Nov. 1968, Avco Everett Research Lab.

[4] Strieff, M. L. and Ferriso, C. C., "Spectral Slit Width of a Small Prism Monochromator," GDA-DBE64-054, Aug. 1964, General Dynamics/Astronautics, Space Science Lab., San Diego, Calif.

[5] "JANAF Thermochemical Tables," The Dow Chemical Company, Midland, Mich.

[6] Wentink, T., "High Temperature Behavior of Teflon," Research Rept. 55, July 1959, Avco Everett Research Lab.

[7] Settlage, P. H. and Siegle, J. C., "Behavior of Teflon Fluorocarbon Resins at Elevated Temperatures," *Planetary and Space Science*, Vol. 3, 1961, pp. 73–81.

[8] Modica, A. P. and Sillers, S. J., "Experimental and Theoretical Kinetics of High-Temperature Fluorocarbon Chemistry," *The Journal of Chemical Physics*, Vol. 48, No. 7, April 1968, pp. 3283–3289.

[9] Gaydon, A. G., *The Spectroscopy of Flames*, Chapman and Hall, London, 1957, Chap. VIII.

[10] Kiess, N. H. and Broida, H. P., *Seventh Symposium on Combustion*, Butterworth, London, 1959, p. 207.

APRIL 1970 AIAA JOURNAL VOL. 8, NO. 4

Failure of Existing Theories to Correlate Experimental Nonacoustic Combustion Instability Data

T. L. Boggs*
Naval Weapons Center, China Lake, Calif.

AND

M. W. Beckstead†
Lockheed Propulsion Company, Redlands, Calif.

Experimental data concerning nonacoustic combustion instability of solid propellants are presented and compared with the predictions of theoretical models. This comparison reveals that the models are inadequate to predict the bulk mode instability behavior of certain propellants such as those using a polyurethane binder. A computational method, the layer frequency concept, is proposed. The results obtained using this technique suggest that the heterogeneity of the propellant and the relationship of the thermal wave thickness to the oxidizer particle sizes are factors that cannot be neglected (as they are in the theoretical models) in the modeling of nonacoustic combustion instability of a propellant system.

Nomenclature

A = nondimensional parameter in the response function (see Ref. 14)
B = nondimensional parameter in the response function (see Ref. 14)
D = oxidizer particle diameter
f = frequency of oscillations, cps
L^* = characteristic length of chamber (free volume divided by nozzle throat area)
$\overline{MW}$ = molecular weight of combustion chamber gases
n = pressure exponent in steady-state burning rate equation $\bar{r} = b\bar{p}^{-n}$
$\bar{p}$ = mean- or time-average pressure
p' = pressure perturbation
$Re\ (\ldots)$ = real part of a complex expression
R = response function $= (r'/\bar{r})/(p'/\bar{p})$
$\bar{r}$ = mean burning rate
r' = burning rate perturbation
T_f = adiabatic flame temperature
x = weight fraction of oxidizer
α = exponential growth rate
α_t = thermal diffusivity of solid
δ = characteristic binder thickness between oxidizer particles
λ = characteristic root of solid phase energy equation (see Eq. 3)
ρ_{ox} = oxidizer density
ρ_f = binder density
τ = characteristic time
τ_{ch} = residence time of the chamber $= c^*L^*\overline{MW}/RT_f$
τ_{tw} = thermal wave relaxation time $= \alpha_t/\bar{r}^2$
Ω = nondimensional frequency $= \alpha_t\omega/\bar{r}^2$
ω = frequency, rad/sec

Presented as Paper 69-175 at the AIAA 7th Aerospace Sciences Meeting, New York, January 20–22, 1969; submitted February 6, 1969, revision received September 8, 1969. This work was supported by NASA under NASA Work Order 6030.

* Research Engineer, Aerothermochemistry Division. Member AIAA.

† Technical Specialist, Engineering Research Department Associate Fellow AIAA.

Introduction

A NUMBER of studies[1–12] have discussed the subject of oscillatory behavior of solid-propellant combustion in low-frequency modes (low compared to acoustic wave modes). Relevant analytical studies[1–4,6] have included modeling of the behavior of the combustor flow system as well as modeling of the perturbation behavior of the propellant combustion. Modeling of the over-all combustion-flow system has been simplified by decoupling the combustor analysis from the combustion zone analysis, using the mass response function as a matching condition to join the two separate analyses.[5] This has permitted better identification of the relationship between nonacoustic instability (NAI) and acoustic instability, and has permitted the relatively well-developed one-dimensional perturbation theory of solid-propellant combustion to be incorporated into the stability analysis for the combustor. These advances permit a much more decisive correlation between theory and the voluminous results of laboratory tests using the L^*-burner[3,5,7,8,10,12] and also advance the possibility of determining whether the experimental results can be used to test the validity of theory. Recently some comparison of this type have been made, which question the validity of the one-dimensional combustion perturbation models.[9–13] The results of the present work with com-